Science Advances
AAAS

Supplementary Materials for

Landmark-modulated directional coding in postrhinal cortex

Patrick A. LaChance, Jalina Graham, Benjamin L. Shapiro, Ashlyn J. Morris, Jeffrey S. Taube*

*Corresponding author. Email: jeffrey.s.taube@dartmouth.edu

Published 28 January 2022, *Sci. Adv.* **8**, eabg8404 (2022)
DOI: 10.1126/sciadv.abg8404

This PDF file includes:

Figs. S1 to S13

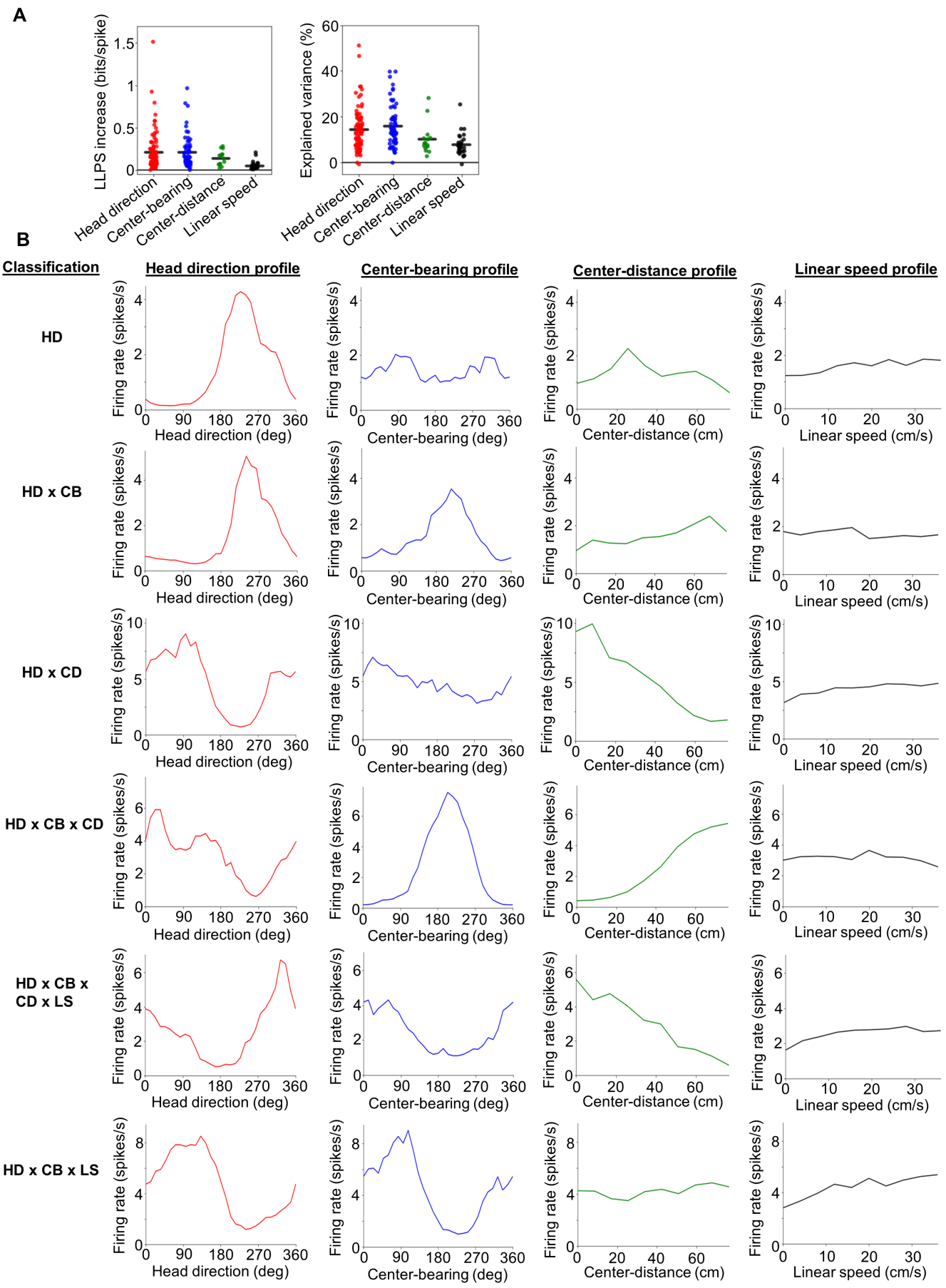
A
LLPS increase (bits/spike)
Explained variance (%)
Head direction
Center-bearing
Center-distance
Linear speed
B
Classification
Head direction profile
Center-bearing profile
Center-distance profile
Linear speed profile
HD
HD x CB
HD x CD
HD x CB x CD
HD x CB x CD x LS
HD x CB x LS
Firing rate (spikes/s)
Head direction (deg)
Center-bearing (deg)
Center-distance (cm)
Linear speed (cm/s)

Figure S1. LM-HD cell tuning to other spatial variables. (A) Goodness-of-fit measures taken from the GLM that show the independent contribution of each variable to the firing rate of each cell tuned to that variable. Strip plots show variable contributions for all 87 LM-HD cells recorded in the A1 session of the AB experiment, but contributions for a given variable are only provided if the cell was classified as encoding that variable. Number of cells classified as belonging to each category: head direction (HD): all 87 cells; center-bearing (CB): 65 cells; center-distance (CD): 15 cells; linear speed (LS): 28 cells. *Left*, contribution calculated using log-likelihood per spike (LLPS) increase. *Right,* contribution calculated using variance explained in the spike train. **(B)** Model-derived response profiles drawn from the GLM for six example LM-HD cells recorded in the A1 session of the AB experiment. Note the variety of variables conjunctively encoded by the cells.

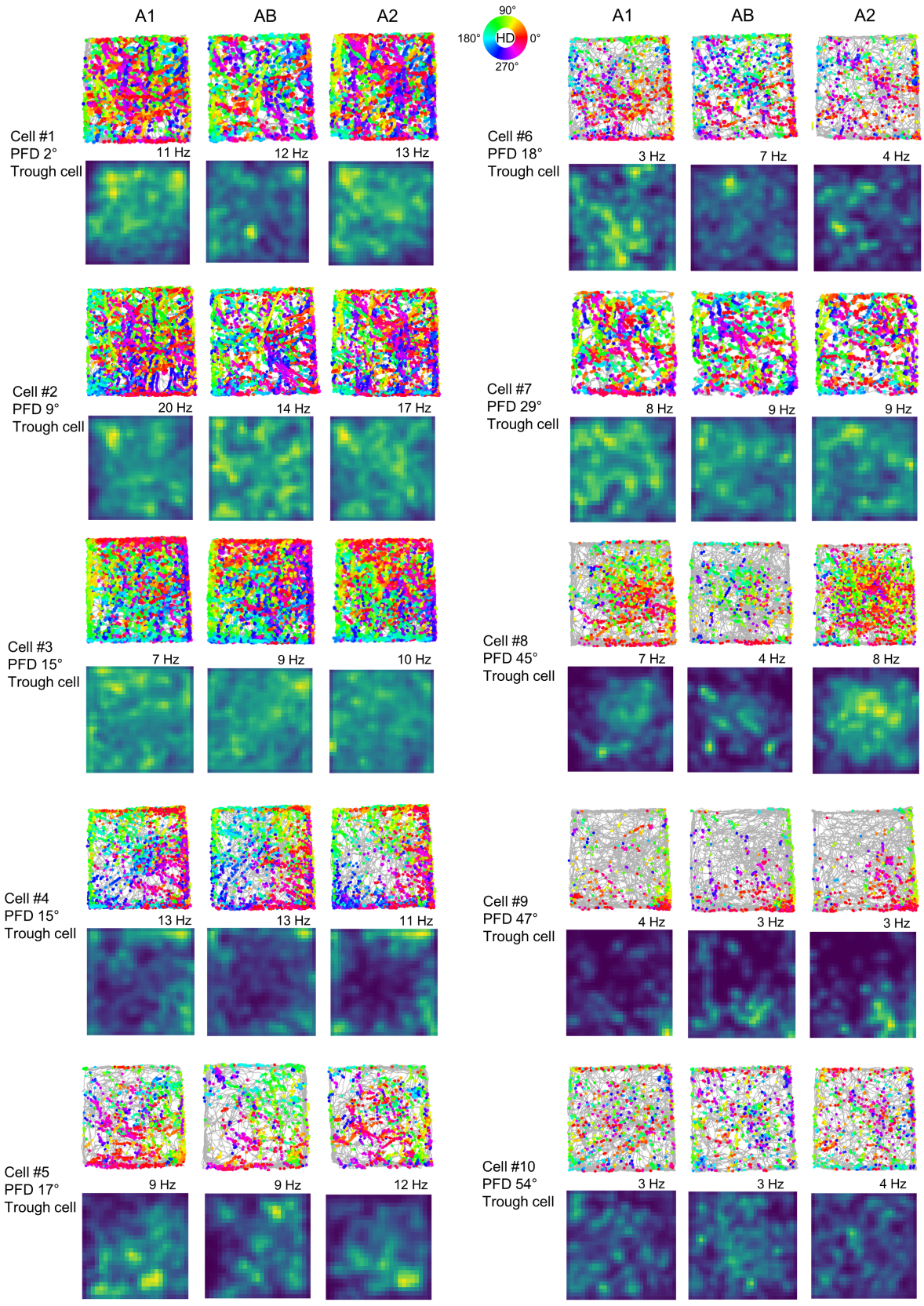
A1
AB
A2
90°
180°
HD
0°
270°
Cell #1
PFD 2°
Trough cell
11 Hz
12 Hz
13 Hz
Cell #2
PFD 9°
Trough cell
20 Hz
14 Hz
17 Hz
Cell #3
PFD 15°
Trough cell
7 Hz
9 Hz
10 Hz
Cell #4
PFD 15°
Trough cell
13 Hz
13 Hz
11 Hz
Cell #5
PFD 17°
Trough cell
9 Hz
9 Hz
12 Hz
Cell #6
PFD 18°
Trough cell
3 Hz
7 Hz
4 Hz
Cell #7
PFD 29°
Trough cell
8 Hz
9 Hz
9 Hz
Cell #8
PFD 45°
Trough cell
7 Hz
4 Hz
8 Hz
Cell #9
PFD 47°
Trough cell
4 Hz
3 Hz
3 Hz
Cell #10
PFD 54°
Trough cell
3 Hz
3 Hz
4 Hz

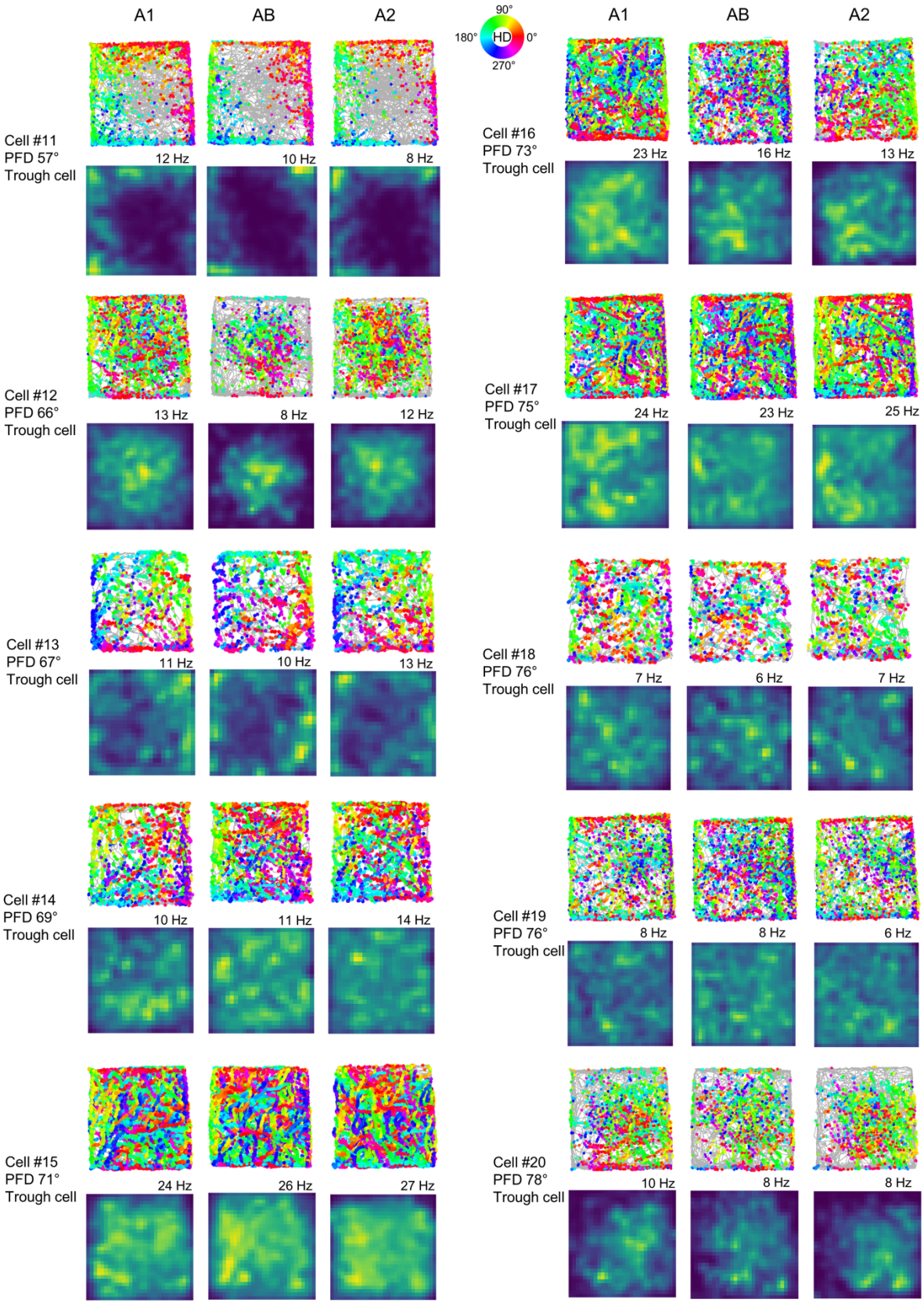
A1
AB
A2
90°
180°
HD
0°
270°
A1
AB
A2
Cell #11
PFD 57°
Trough cell
12 Hz
10 Hz
8 Hz
Cell #16
PFD 73°
Trough cell
23 Hz
16 Hz
13 Hz
Cell #12
PFD 66°
Trough cell
13 Hz
8 Hz
12 Hz
Cell #17
PFD 75°
Trough cell
24 Hz
23 Hz
25 Hz
Cell #13
PFD 67°
Trough cell
11 Hz
10 Hz
13 Hz
Cell #18
PFD 76°
Trough cell
7 Hz
6 Hz
7 Hz
Cell #14
PFD 69°
Trough cell
10 Hz
11 Hz
14 Hz
Cell #19
PFD 76°
Trough cell
8 Hz
8 Hz
6 Hz
Cell #15
PFD 71°
Trough cell
24 Hz
26 Hz
27 Hz
Cell #20
PFD 78°
Trough cell
10 Hz
8 Hz
8 Hz

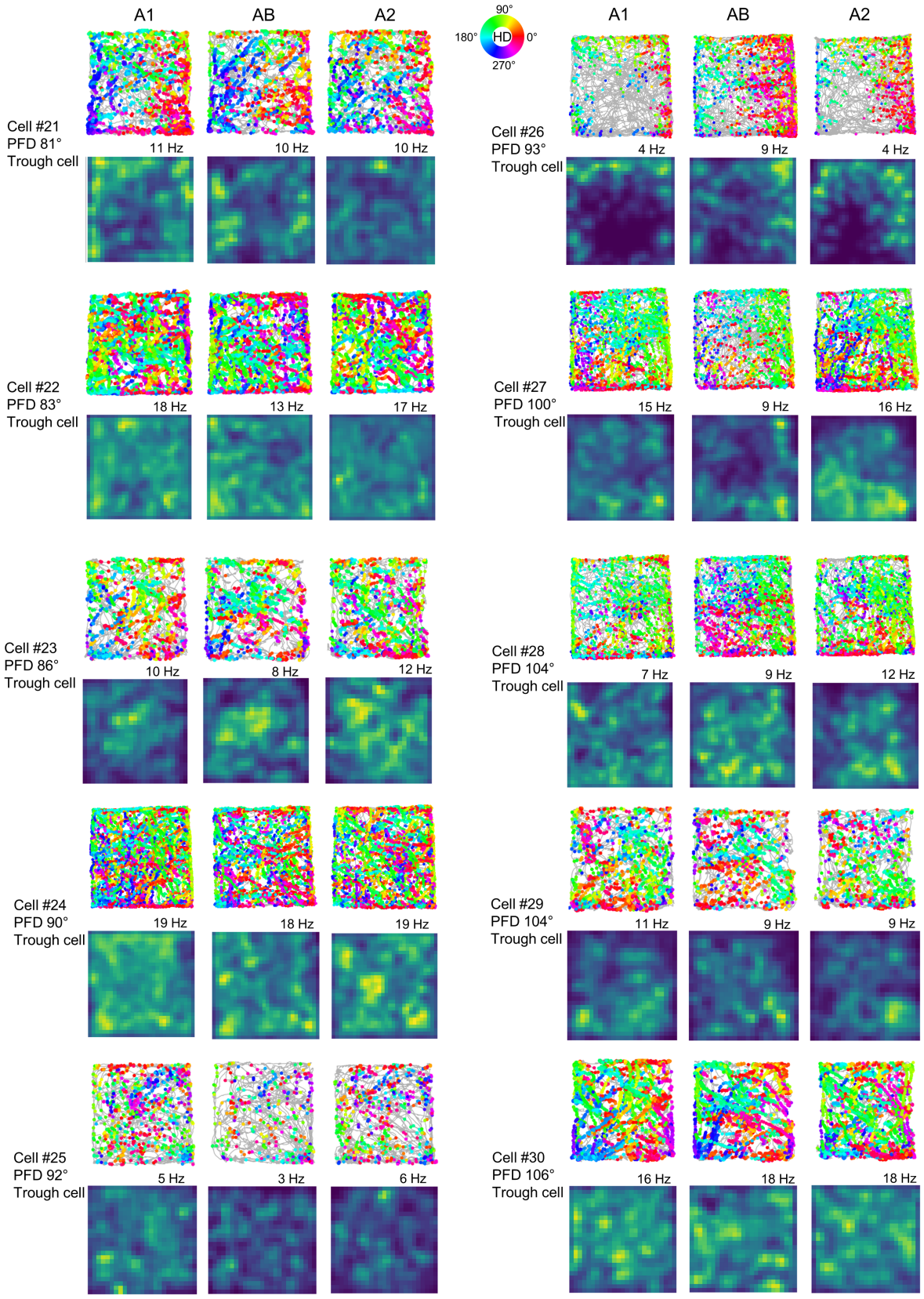
A1
AB
A2
90°
180°
HD
0°
270°
Cell #21
PFD 81°
Trough cell
11 Hz
10 Hz
10 Hz
Cell #22
PFD 83°
Trough cell
18 Hz
13 Hz
17 Hz
Cell #23
PFD 86°
Trough cell
10 Hz
8 Hz
12 Hz
Cell #24
PFD 90°
Trough cell
19 Hz
18 Hz
19 Hz
Cell #25
PFD 92°
Trough cell
5 Hz
3 Hz
6 Hz
Cell #26
PFD 93°
Trough cell
4 Hz
9 Hz
4 Hz
Cell #27
PFD 100°
Trough cell
15 Hz
9 Hz
16 Hz
Cell #28
PFD 104°
Trough cell
7 Hz
9 Hz
12 Hz
Cell #29
PFD 104°
Trough cell
11 Hz
9 Hz
9 Hz
Cell #30
PFD 106°
Trough cell
16 Hz
18 Hz
18 Hz

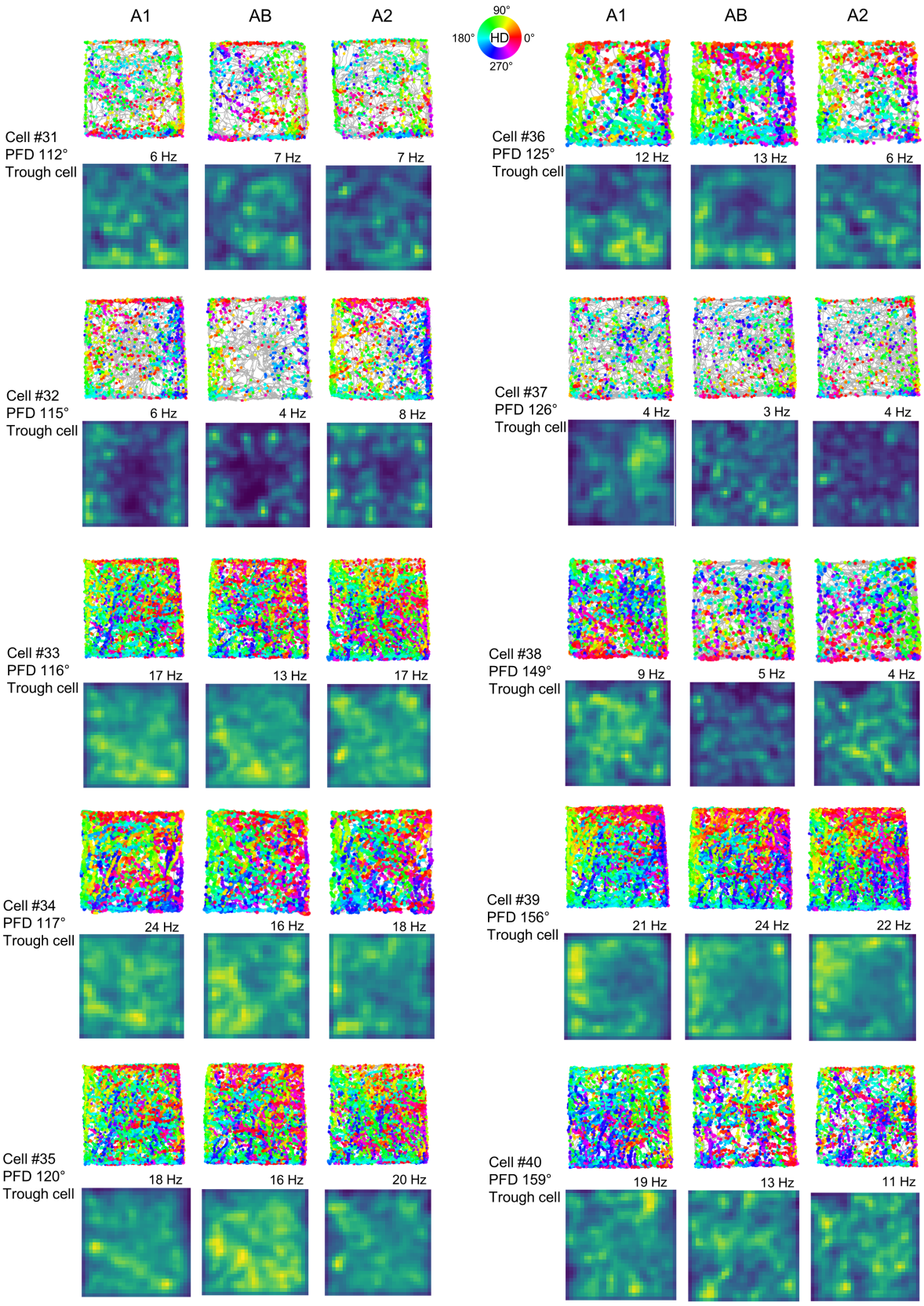
A1
AB
A2
90°
180°
HD
0°
270°
Cell #31
PFD 112°
Trough cell
6 Hz
7 Hz
7 Hz
Cell #36
PFD 125°
Trough cell
12 Hz
13 Hz
6 Hz
Cell #32
PFD 115°
Trough cell
6 Hz
4 Hz
8 Hz
Cell #37
PFD 126°
Trough cell
4 Hz
3 Hz
4 Hz
Cell #33
PFD 116°
Trough cell
17 Hz
13 Hz
17 Hz
Cell #38
PFD 149°
Trough cell
9 Hz
5 Hz
4 Hz
Cell #34
PFD 117°
Trough cell
24 Hz
16 Hz
18 Hz
Cell #39
PFD 156°
Trough cell
21 Hz
24 Hz
22 Hz
Cell #35
PFD 120°
Trough cell
18 Hz
16 Hz
20 Hz
Cell #40
PFD 159°
Trough cell
19 Hz
13 Hz
11 Hz

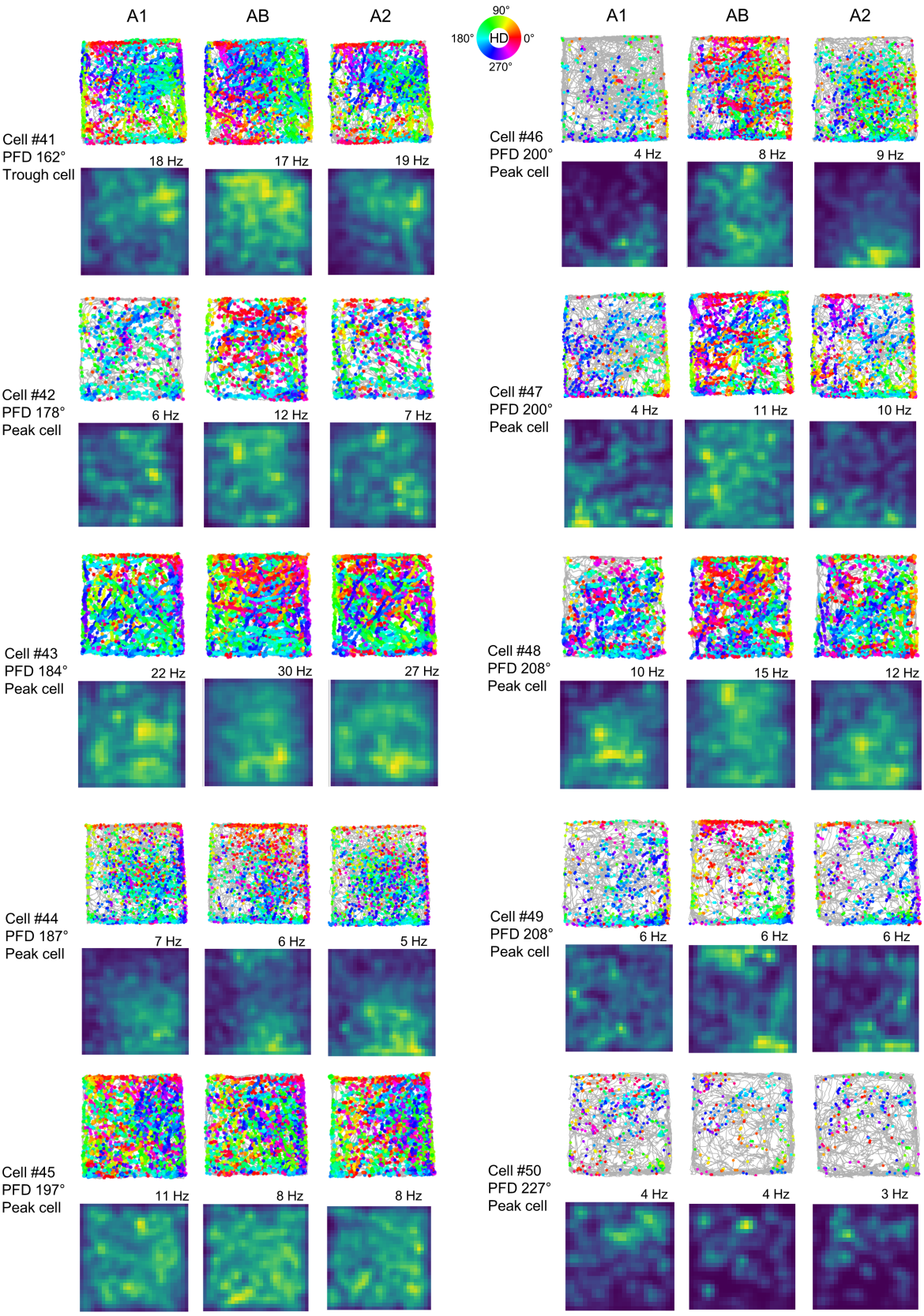
A1
AB
A2
90°
180°
HD
0°
270°
Cell #41
PFD 162°
Trough cell
18 Hz
17 Hz
19 Hz
Cell #42
PFD 178°
Peak cell
6 Hz
12 Hz
7 Hz
Cell #43
PFD 184°
Peak cell
22 Hz
30 Hz
27 Hz
Cell #44
PFD 187°
Peak cell
7 Hz
6 Hz
5 Hz
Cell #45
PFD 197°
Peak cell
11 Hz
8 Hz
8 Hz
A1
AB
A2
Cell #46
PFD 200°
Peak cell
4 Hz
8 Hz
9 Hz
Cell #47
PFD 200°
Peak cell
4 Hz
11 Hz
10 Hz
Cell #48
PFD 208°
Peak cell
10 Hz
15 Hz
12 Hz
Cell #49
PFD 208°
Peak cell
6 Hz
6 Hz
6 Hz
Cell #50
PFD 227°
Peak cell
4 Hz
4 Hz
3 Hz

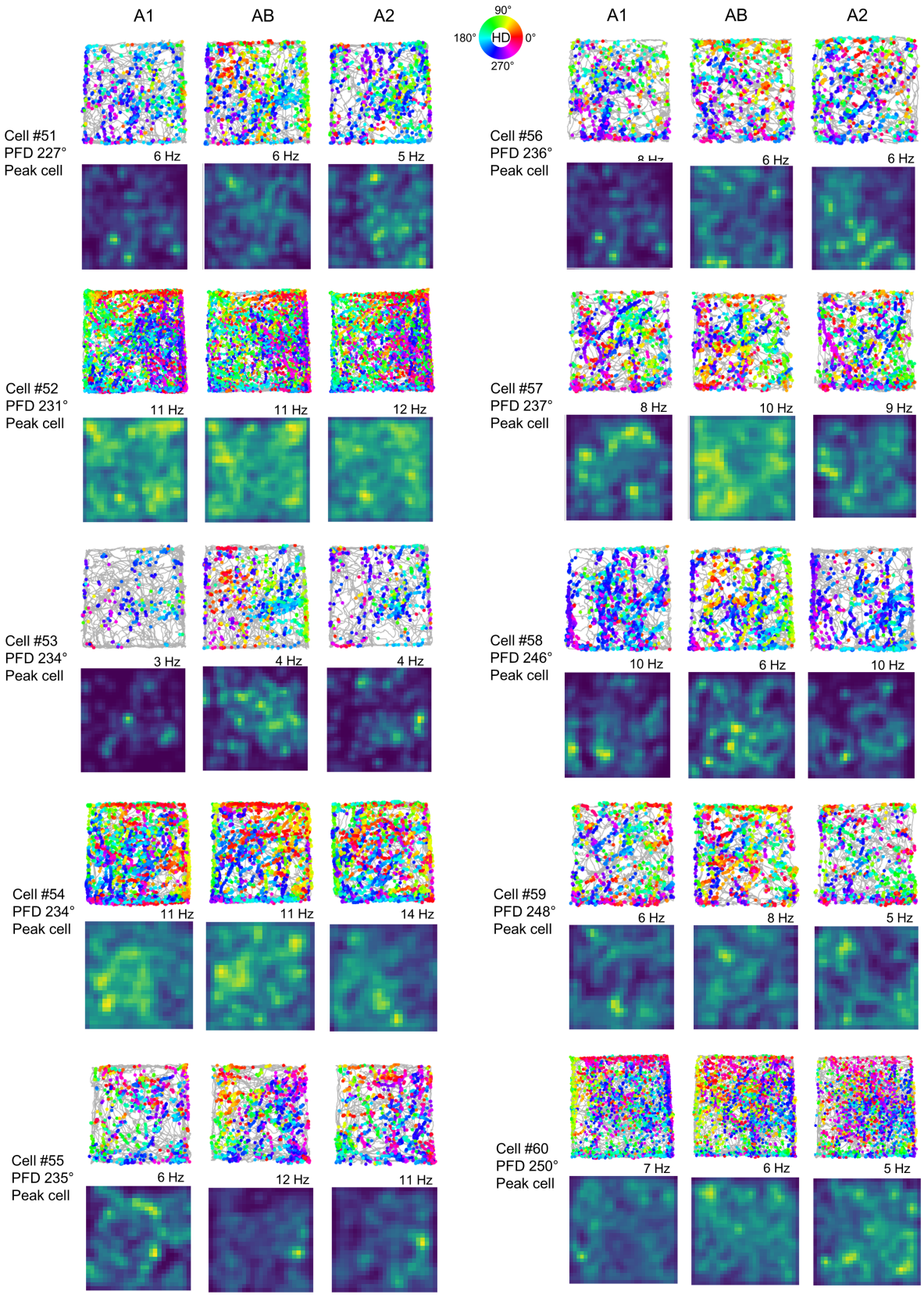
A1
AB
A2
90°
180°
HD
0°
270°
Cell #51
PFD 227°
Peak cell
6 Hz
6 Hz
5 Hz
Cell #52
PFD 231°
Peak cell
11 Hz
11 Hz
12 Hz
Cell #53
PFD 234°
Peak cell
3 Hz
4 Hz
4 Hz
Cell #54
PFD 234°
Peak cell
11 Hz
11 Hz
14 Hz
Cell #55
PFD 235°
Peak cell
6 Hz
12 Hz
11 Hz
A1
AB
A2
Cell #56
PFD 236°
Peak cell
6 Hz
6 Hz
Cell #57
PFD 237°
Peak cell
8 Hz
10 Hz
9 Hz
Cell #58
PFD 246°
Peak cell
10 Hz
6 Hz
10 Hz
Cell #59
PFD 248°
Peak cell
6 Hz
8 Hz
5 Hz
Cell #60
PFD 250°
Peak cell
7 Hz
6 Hz
5 Hz

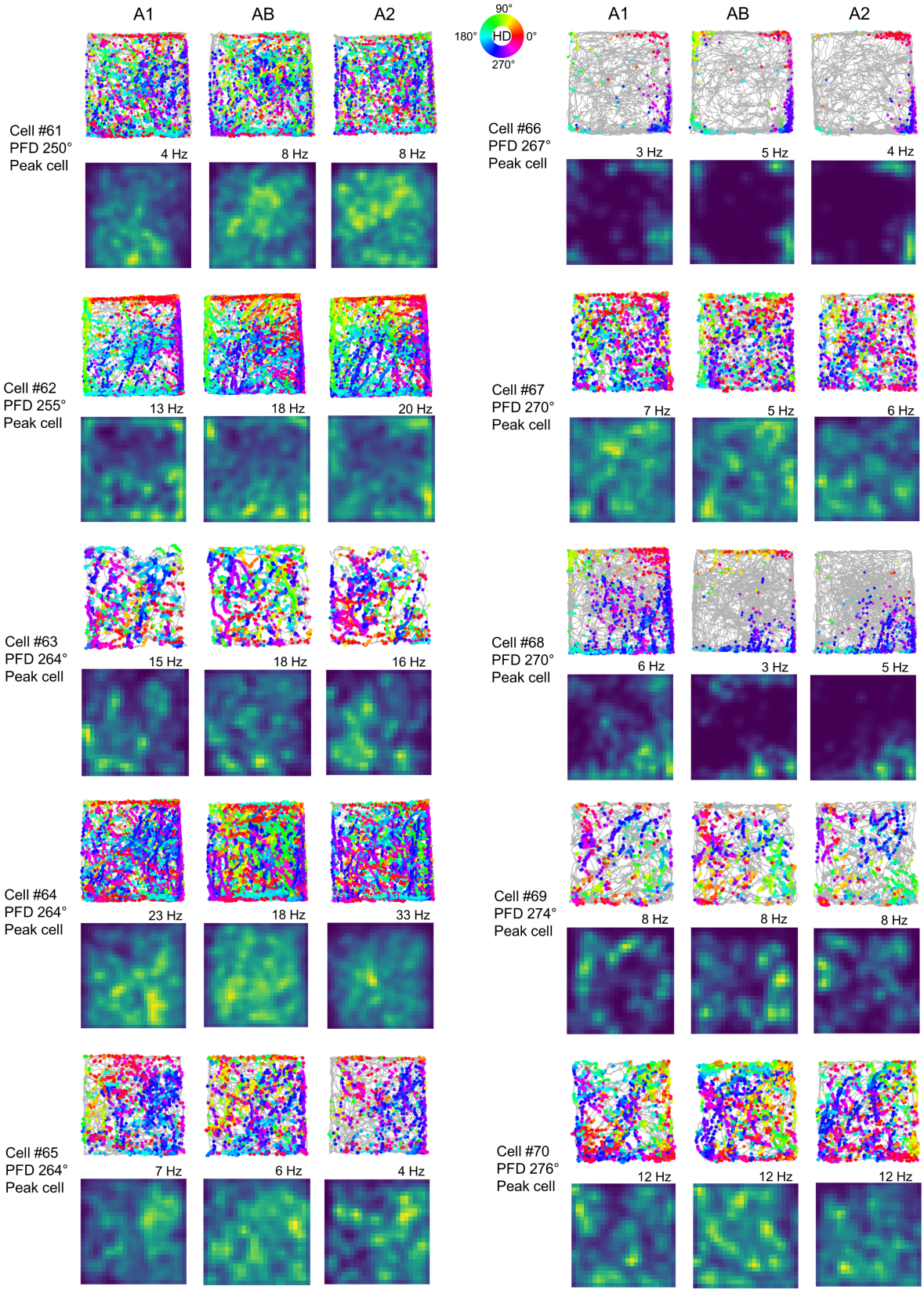
A1
AB
A2
90°
180°
HD
0°
270°
Cell #61
PFD 250°
Peak cell
4 Hz
8 Hz
8 Hz
Cell #66
PFD 267°
Peak cell
3 Hz
5 Hz
4 Hz
Cell #62
PFD 255°
Peak cell
13 Hz
18 Hz
20 Hz
Cell #67
PFD 270°
Peak cell
7 Hz
5 Hz
6 Hz
Cell #63
PFD 264°
Peak cell
15 Hz
18 Hz
16 Hz
Cell #68
PFD 270°
Peak cell
6 Hz
3 Hz
5 Hz
Cell #64
PFD 264°
Peak cell
23 Hz
18 Hz
33 Hz
Cell #69
PFD 274°
Peak cell
8 Hz
8 Hz
8 Hz
Cell #65
PFD 264°
Peak cell
7 Hz
6 Hz
4 Hz
Cell #70
PFD 276°
Peak cell
12 Hz
12 Hz
12 Hz

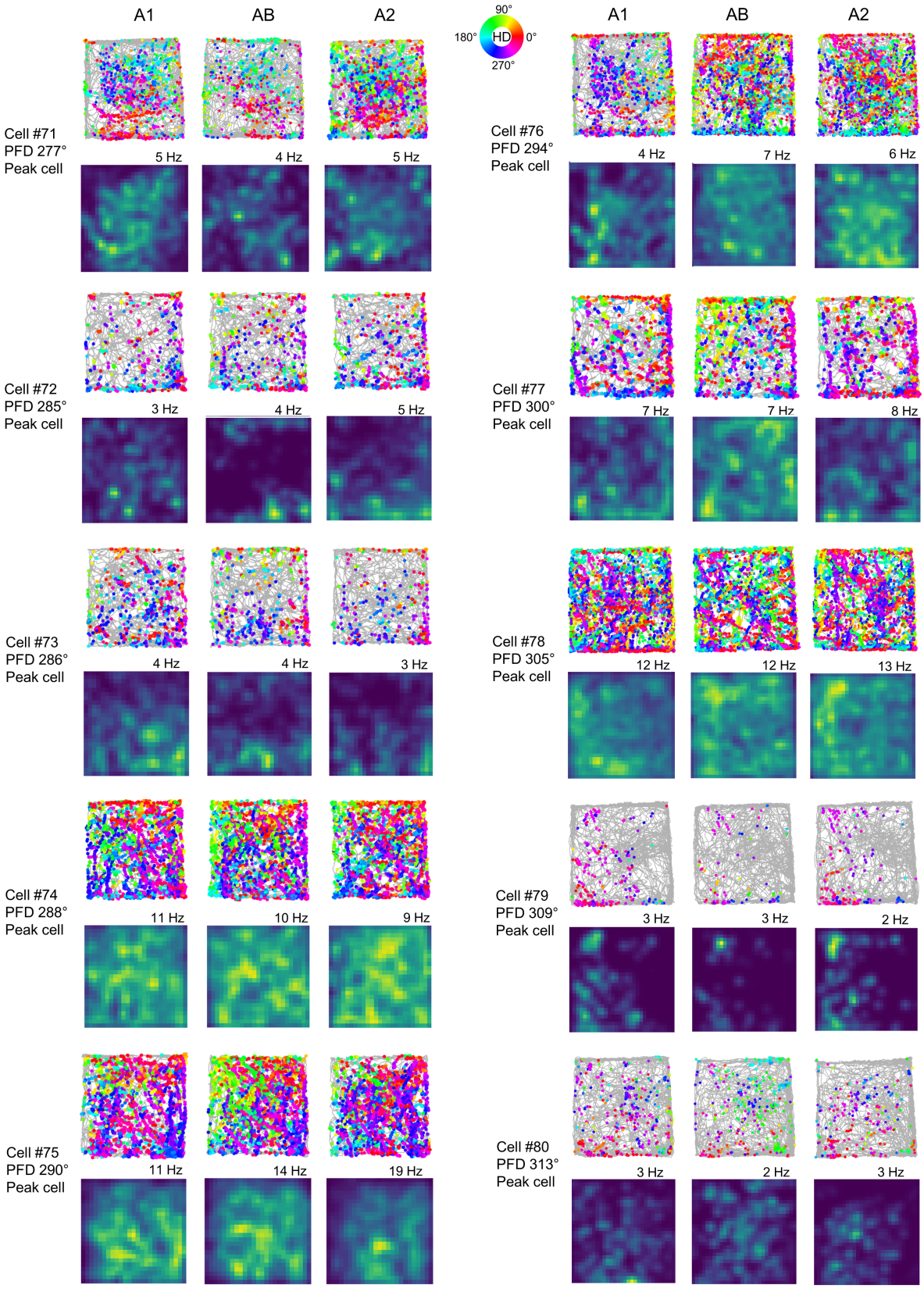
A1
AB
A2
90°
180°
HD
0°
270°
Cell #71
PFD 277°
Peak cell
5 Hz
4 Hz
5 Hz
Cell #76
PFD 294°
Peak cell
4 Hz
7 Hz
6 Hz
Cell #72
PFD 285°
Peak cell
3 Hz
4 Hz
5 Hz
Cell #77
PFD 300°
Peak cell
7 Hz
7 Hz
8 Hz
Cell #73
PFD 286°
Peak cell
4 Hz
4 Hz
3 Hz
Cell #78
PFD 305°
Peak cell
12 Hz
12 Hz
13 Hz
Cell #74
PFD 288°
Peak cell
11 Hz
10 Hz
9 Hz
Cell #79
PFD 309°
Peak cell
3 Hz
3 Hz
2 Hz
Cell #75
PFD 290°
Peak cell
11 Hz
14 Hz
19 Hz
Cell #80
PFD 313°
Peak cell
3 Hz
2 Hz
3 Hz

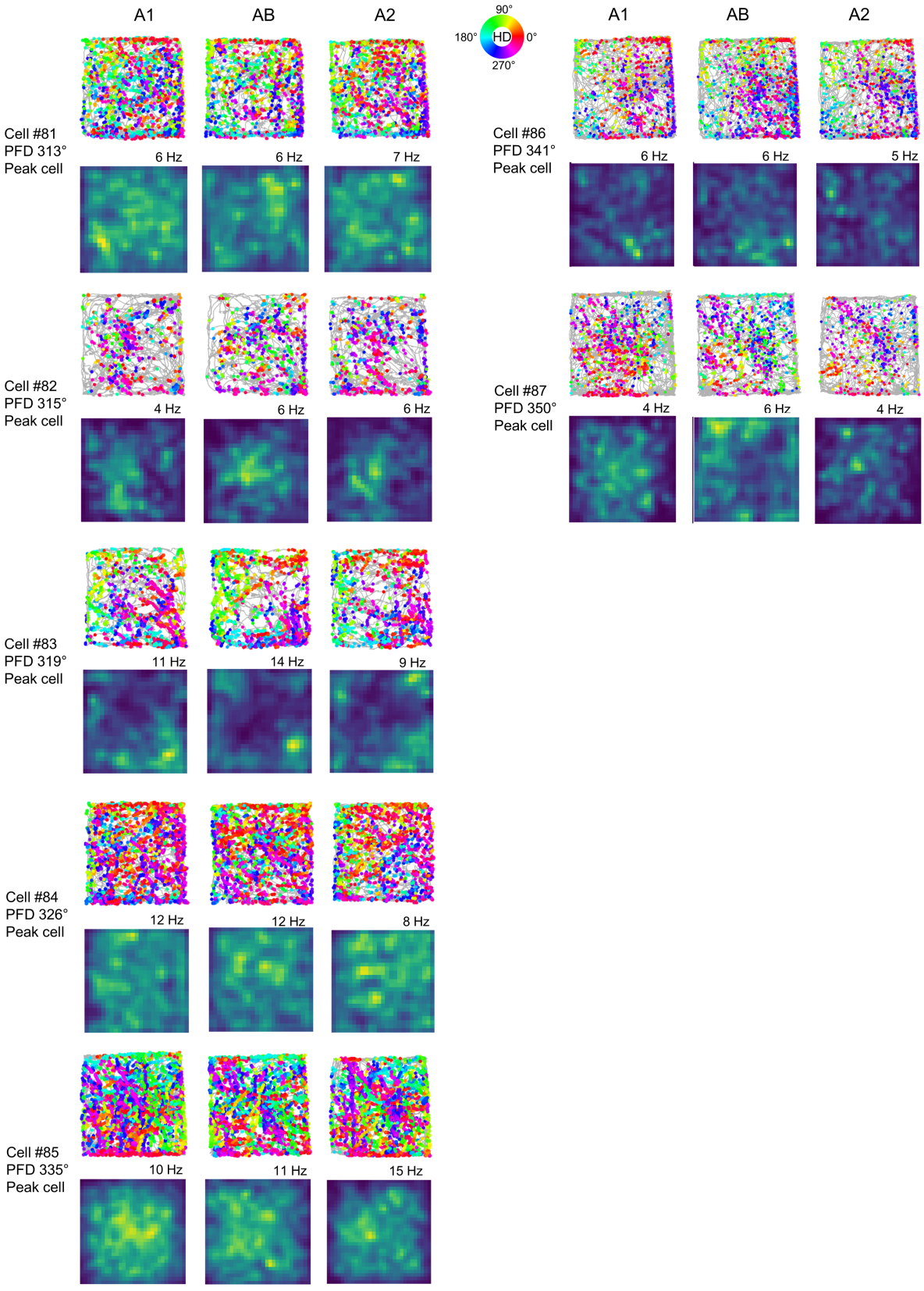
A1
AB
A2
90°
180°
HD
0°
270°
Cell #81
PFD 313°
Peak cell
6 Hz
6 Hz
7 Hz
Cell #82
PFD 315°
Peak cell
4 Hz
6 Hz
6 Hz
Cell #83
PFD 319°
Peak cell
11 Hz
14 Hz
9 Hz
Cell #84
PFD 326°
Peak cell
12 Hz
12 Hz
8 Hz
Cell #85
PFD 335°
Peak cell
10 Hz
11 Hz
15 Hz
Cell #86
PFD 341°
Peak cell
6 Hz
6 Hz
5 Hz
Cell #87
PFD 350°
Peak cell
4 Hz
6 Hz
4 Hz

Figure S2. AB session trajectories and rate maps. Directional spike plots and spatial heatmaps for all 87 POR LM-HD cells recorded across the three sessions of the AB experiment, ordered according to their PFD in the A1 session (same as order in Fig. 1F). Number above each heatmap indicates the maximum firing rate.

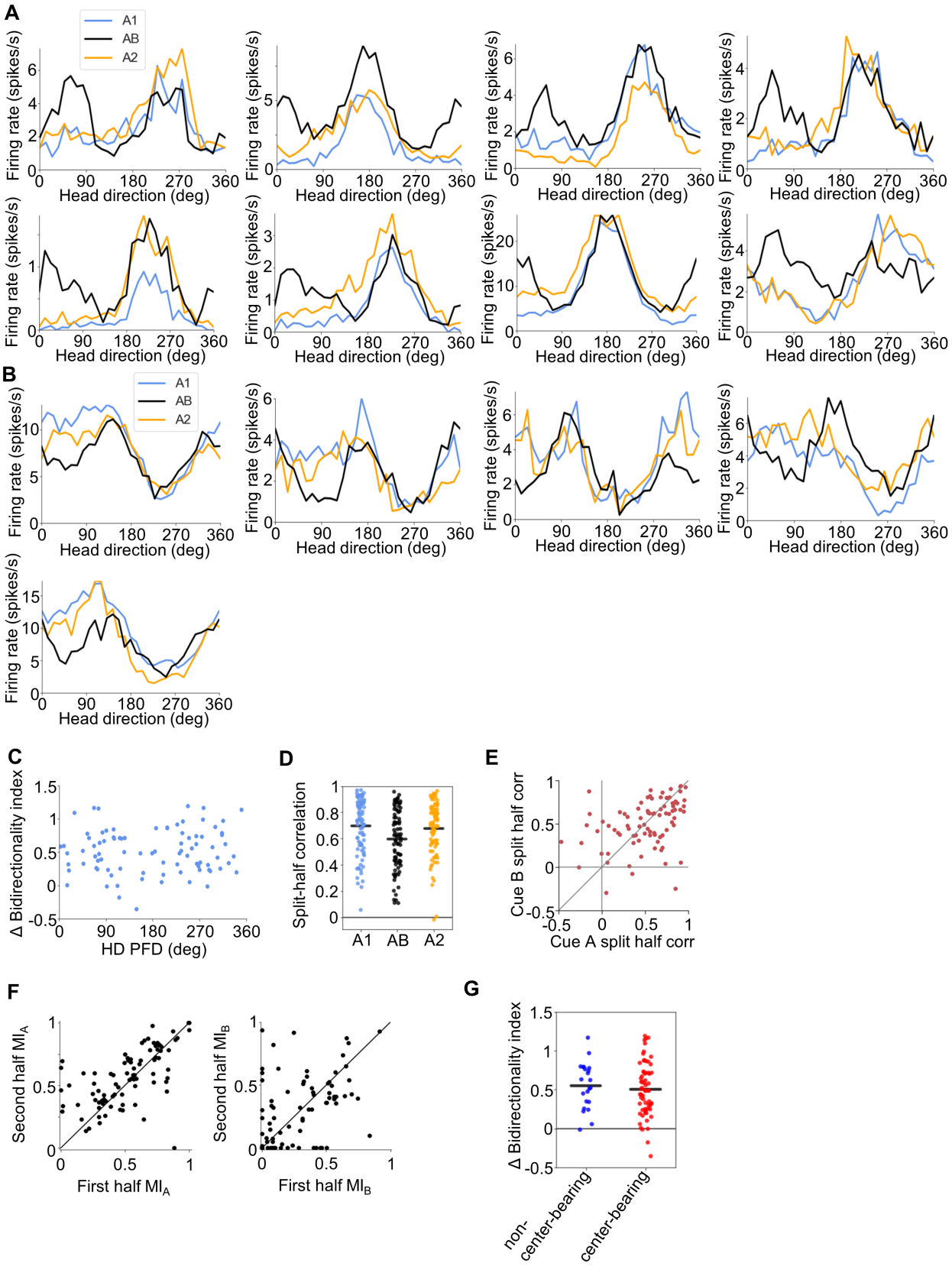
A
A1
AB
A2
Firing rate (spikes/s)
Head direction (deg)
0 90 180 270 360
B
C
Δ Bidirectionality index
HD PFD (deg)
D
Split-half correlation
A1 AB A2
E
Cue B split half corr
Cue A split half corr
F
Second half MI$_A$
First half MI$_A$
Second half MI$_B$
First half MI$_B$
G
Δ Bidirectionality index
non-center-bearing
center-bearing

Figure S3. AB session additional data – POR. (A) Tuning curves for eight example POR LM-HD cells recorded in the AB experiment that displayed 'peak-locked' tuning. **(B)** Tuning curves for five example POR LM-HD cells that displayed 'trough-locked' tuning. **(C)** Comparison of bidirectionality index for all LM-HD cells recorded during the AB session with their HD PFDs from the A1 session. **(D)** Split-half correlations for all LM-HD cells across the three sessions of the AB experiment. **(E)** Split-half correlations for all LM-HD cells recorded in the AB session separated into the portion of the tuning curve related to cue A vs. cue B. Diagonal line shows x = y. **(F)** Comparison of tuning strength relative to cue A (*left*) or cue B (*right*) using modulation index (MI) across both halves of the AB session for all LM-HD cells recorded in the AB session. **(G)** Comparison of change in bidirectionality index from A1 to AB for LM-HD cells tuned conjunctively to center-bearing (CB; 65 cells) or not (non-CB; 22 cells).

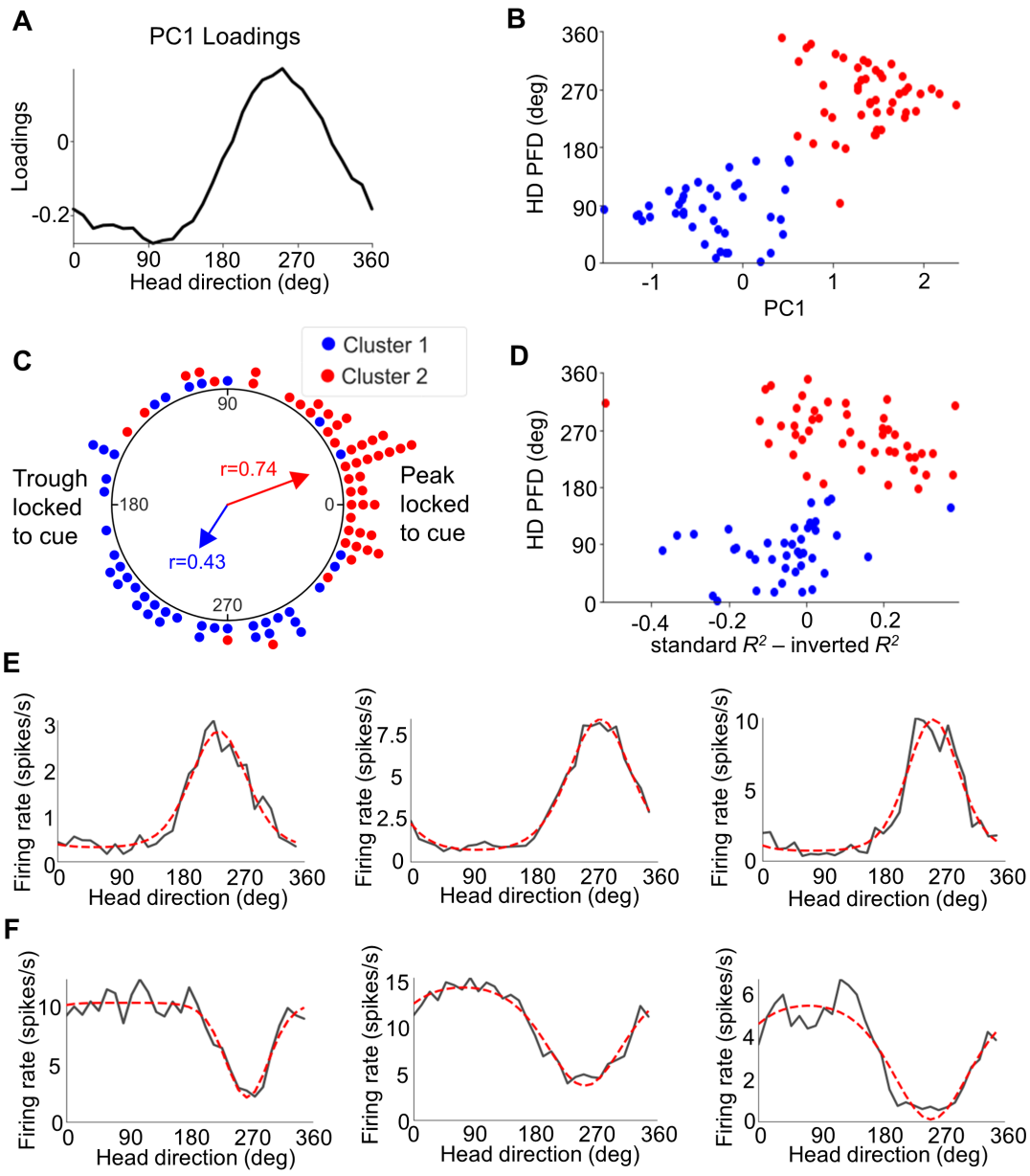

Figure S4. Principal component analysis, clustering, and von Mises fits. (A) Loadings for PC1. Note that PC1 roughly identifies whether a cell's tuning curve has a firing rate maximum or minimum near 270°. **(B)** Scatter plot depicting the relationship between each cell's A1 PFD and the PC1 score of its tuning curve. Note that cells with PFDs near 270° tend to have positive scores, while cells with PFDs closer to 90° have negative scores. Clusters are the result of k-means clustering using the first two principal components. **(C)** Polar dot plot showing the difference between each cell's A1 PFD (doubled and remainder taken from 360°) and its AB angle-doubled PFD. Differences near 0° mean that firing rate maxima were aligned between A1 and AB sessions (i.e. peak-locked tuning). Differences near 180° mean that the A1 maximum

firing rate was displaced by a new firing rate minimum in the AB session (i.e. trough-locked tuning). Cluster 1 tends to show trough-locked tuning, while cluster 2 shows peak-locked tuning. **(D)** Scatter plot showing relationship between each cell's A1 PFD and the fit of its tuning curve by either an upright or inverted von Mises distribution. Clusters are the result of k-means clustering based on both PFD and R^2 fit difference. Note that these clusters are nearly identical to those derived from PCA. **(E)** Tuning curves and upright von Mises fits for three POR LM-HD cells that showed better fits by an upright distribution. **(F)** Tuning curves and inverted von Mises fits for three POR LM-HD cells that showed better fits by an inverted distribution.

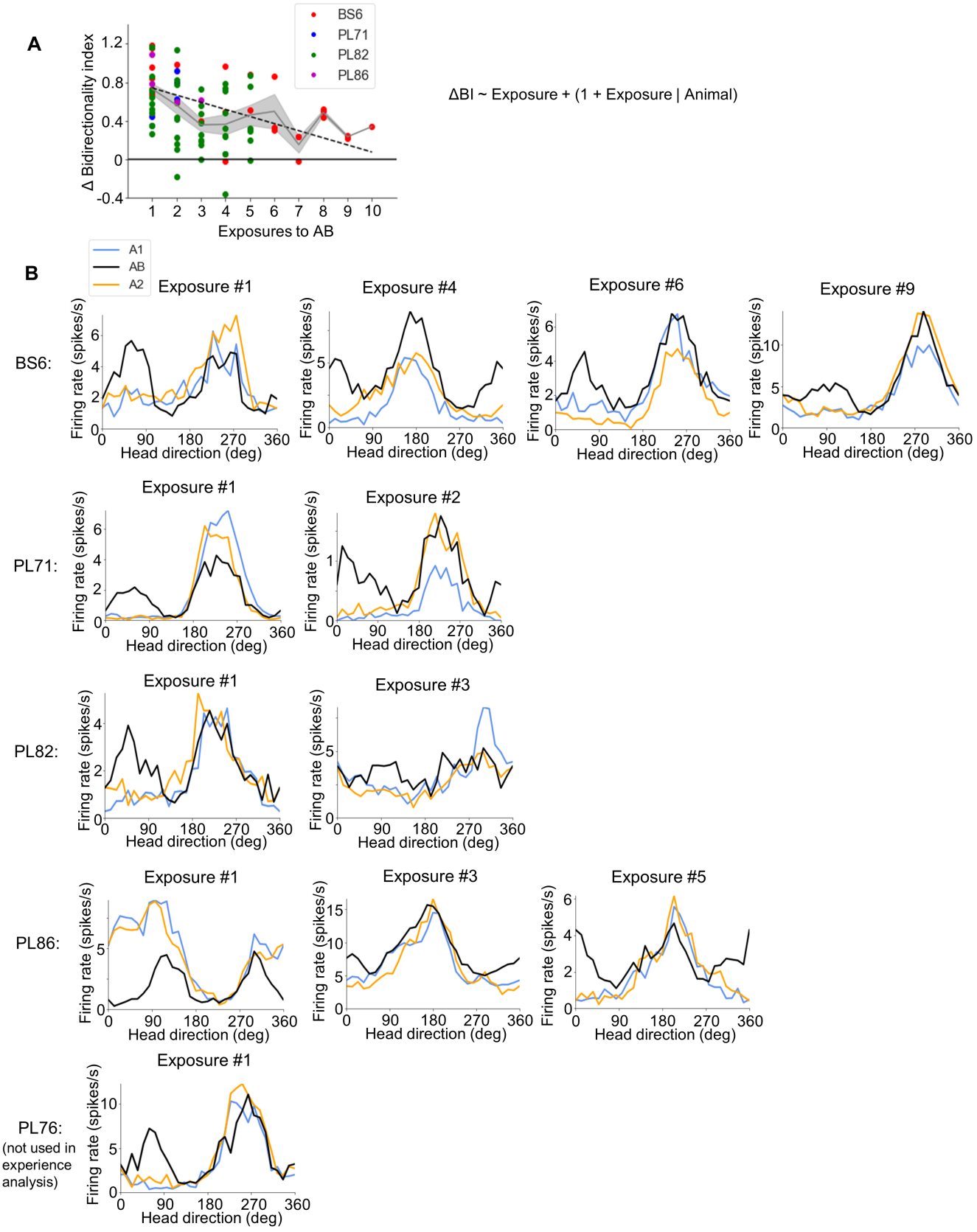
A
BS6
PL71
PL82
PL86
Δ Bidirectionality index
Exposures to AB
ΔBI ~ Exposure + (1 + Exposure | Animal)
B
A1
AB
A2
BS6:
PL71:
PL82:
PL86:
PL76:
(not used in experience analysis)
Exposure #1
Exposure #2
Exposure #3
Exposure #4
Exposure #5
Exposure #6
Exposure #9
Firing rate (spikes/s)
Head direction (deg)

Figure S5. Decrease in bidirectionality with repeated exposures to AB session. (A) Plot showing the change in bidirectionality index from A1 to AB for all 87 LM-HD cells recorded in the AB experiment, colored by animal and ordered by how many times the animal had experienced the AB configuration. Gray line and error bars show mean and SEM for LM-HD cells recorded during each exposure. Dotted black line shows the linear mixed model fit for the effect of exposure number on change in bidirectionality index (model formula noted to the right). Exposure to AB was found to have a significant negative effect on bidirectionality over time, although bidirectionality was still present after up to 10 exposures **(B)** Tuning curves for POR LM-HD cells recorded in the three sessions of the AB experiment from all five animals used in the experiment. Multiple plots are shown for animals that had multiple exposures to the environment (all but PL76 who was excluded from the exposure analysis due to only having one exposure).

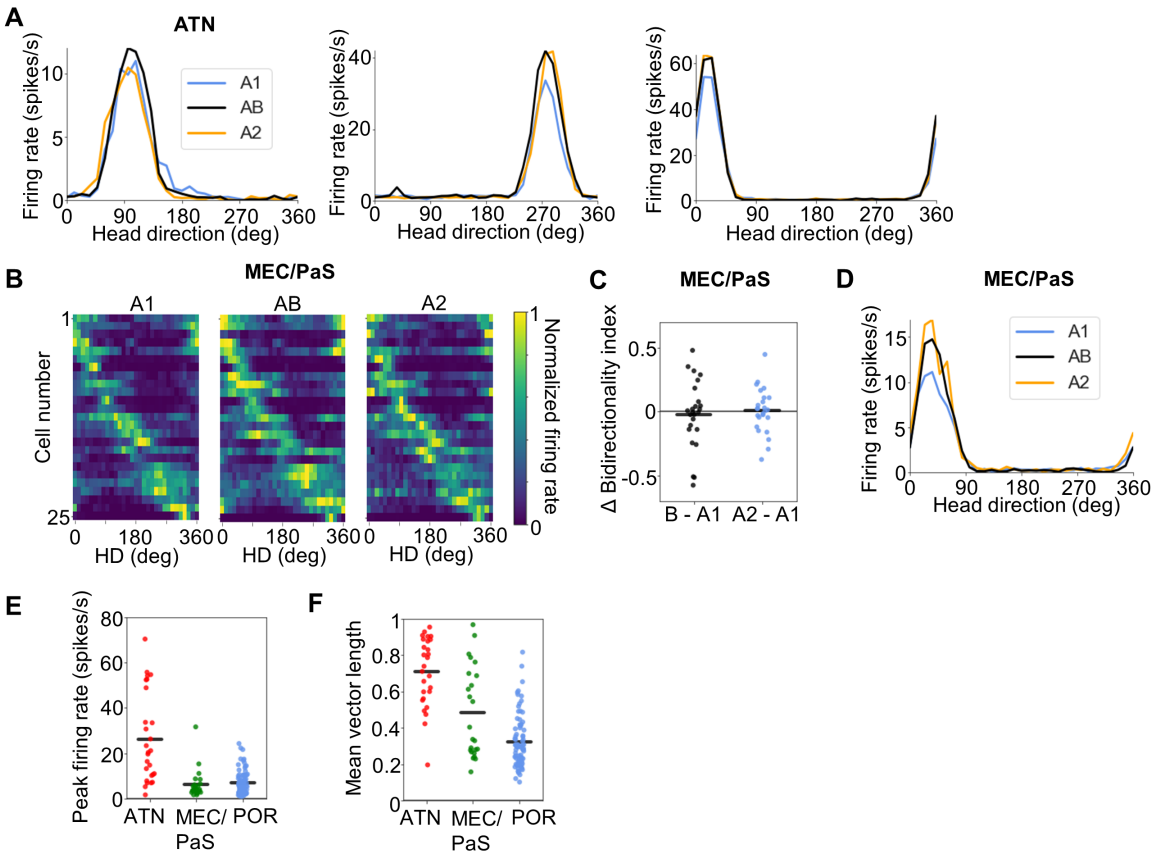

Figure S6. AB session additional data – ATN and MEC/PaS. (A) Tuning curves for three example ATN HD cells recorded in the AB experiment. **(B)** Normalized tuning curves for 25 MEC/PaS HD cells recorded across A1-AB-A2 sessions. **(C)** Comparison of bidirectionality index between A1 and both AB and A2 sessions for MEC/PaS cells, showing no change in bidirectionality. **(D)** Tuning curves for an example cell recorded from MEC/PaS across A1, AB, and A2 sessions. **(E)** Comparison of peak firing rates for LM-HD or HD cells recorded in the A1 session of the AB experiment from ATN, MEC/PaS, and POR. **(F)** Same as (E) but for mean vector lengths.

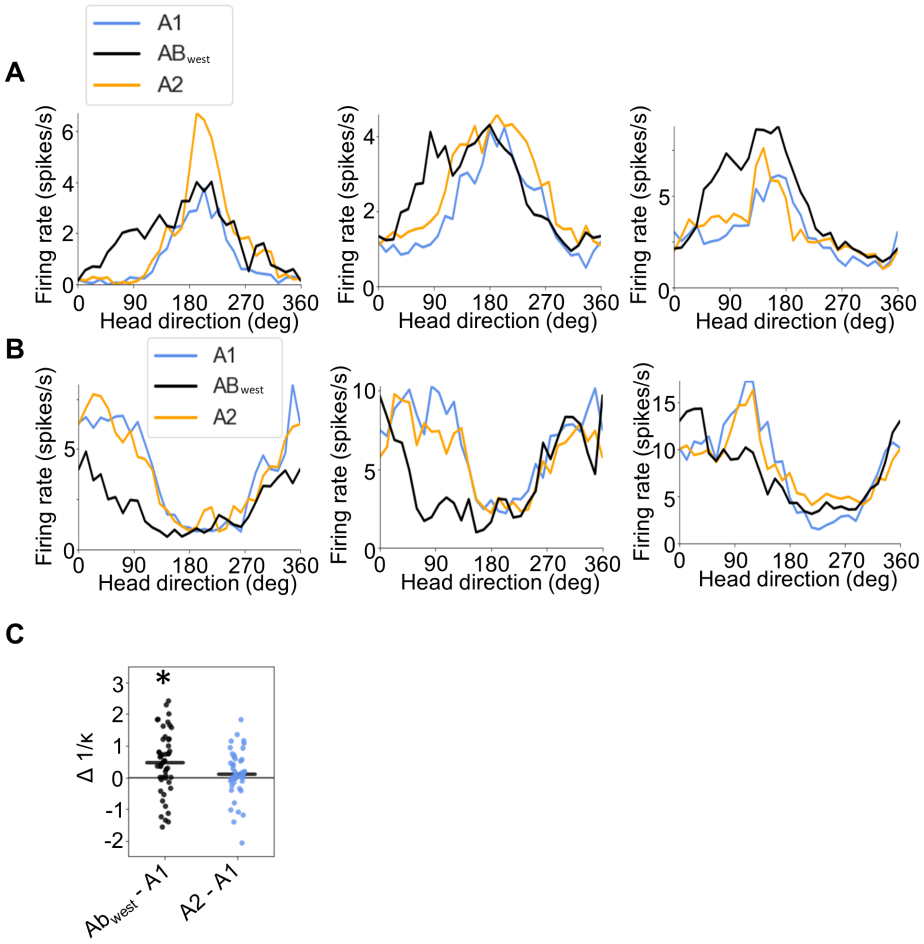

Figure S7. AB_{west} session additional data. (A) Tuning curves for three example POR LM-HD cells recorded in the AB_{west} experiment that displayed 'peak-locked' tuning. Note the broadening of the peak in the clockwise direction **(B)** Tuning curves for three example POR LM-HD cells that displayed 'trough-locked' tuning. Note the broadening of the trough in the clockwise direction. **(C)** Comparison of 1/κ concentration values for unimodal von Mises distributions fit to HD tuning curves between the A1 session and both AB_{west} and A2 sessions. * denotes significance.

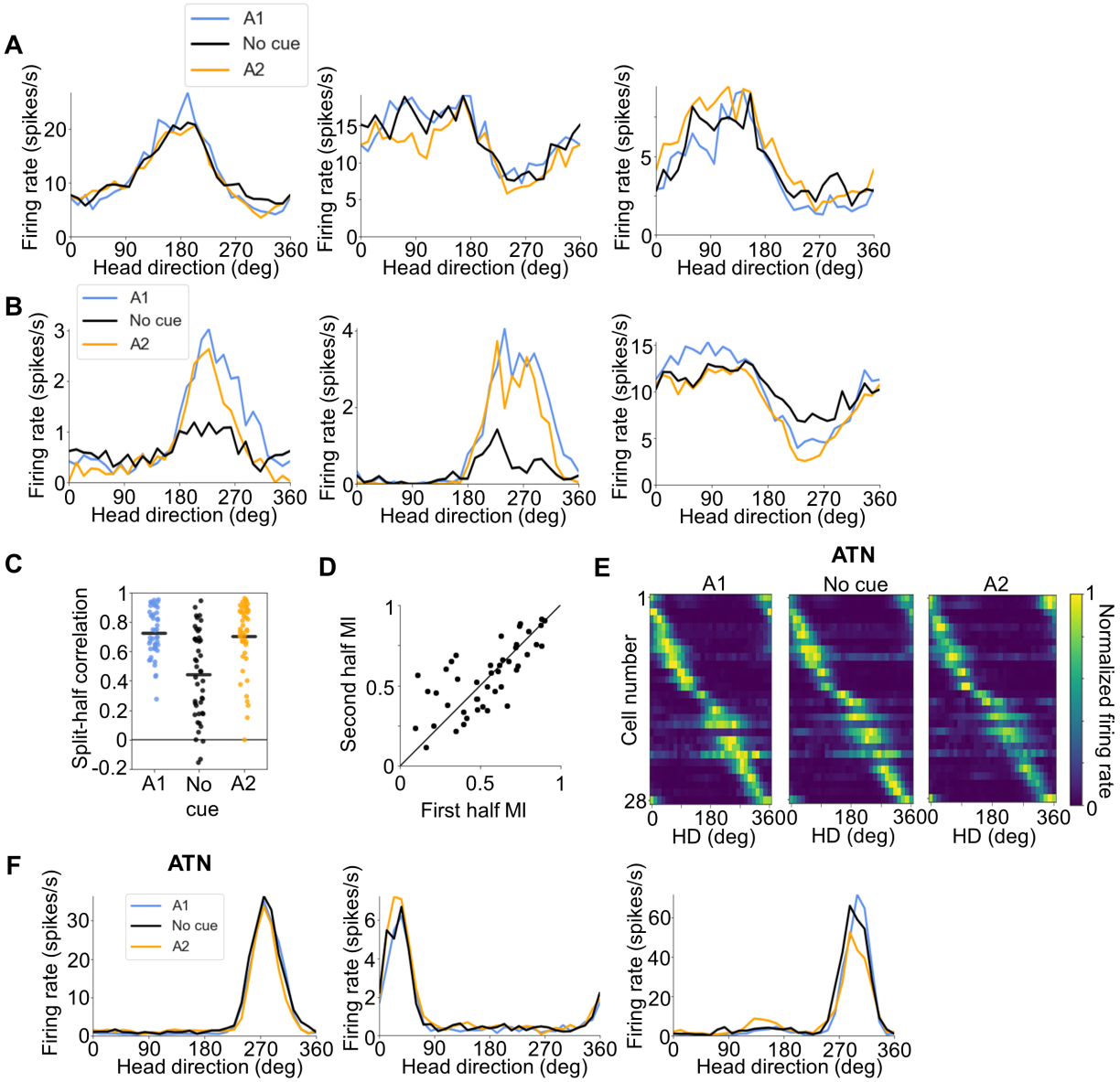

Figure S8. No cue session additional data. (A) Tuning curves for three example POR LM-HD cells that maintained their tuning properties during the No cue session. **(B)** Tuning curves for three example POR LM-HD cells that showed marked tuning degradation during the No cue session (*left, middle*: cells with positive peak tuning; *right*: cell with trough tuning). **(C)** Comparison of split-half correlations for all LM-HD cells recorded across the three sessions of the No cue experiment **(D)** Comparison of tuning strength relative to cue A (measured using modulation index) across both halves of the No cue session. **(E)** Normalized tuning curves for all ATN HD cells recorded in the No cue experiment. **(F)** Tuning curves for three example ATN HD cells recorded in the No cue experiment.

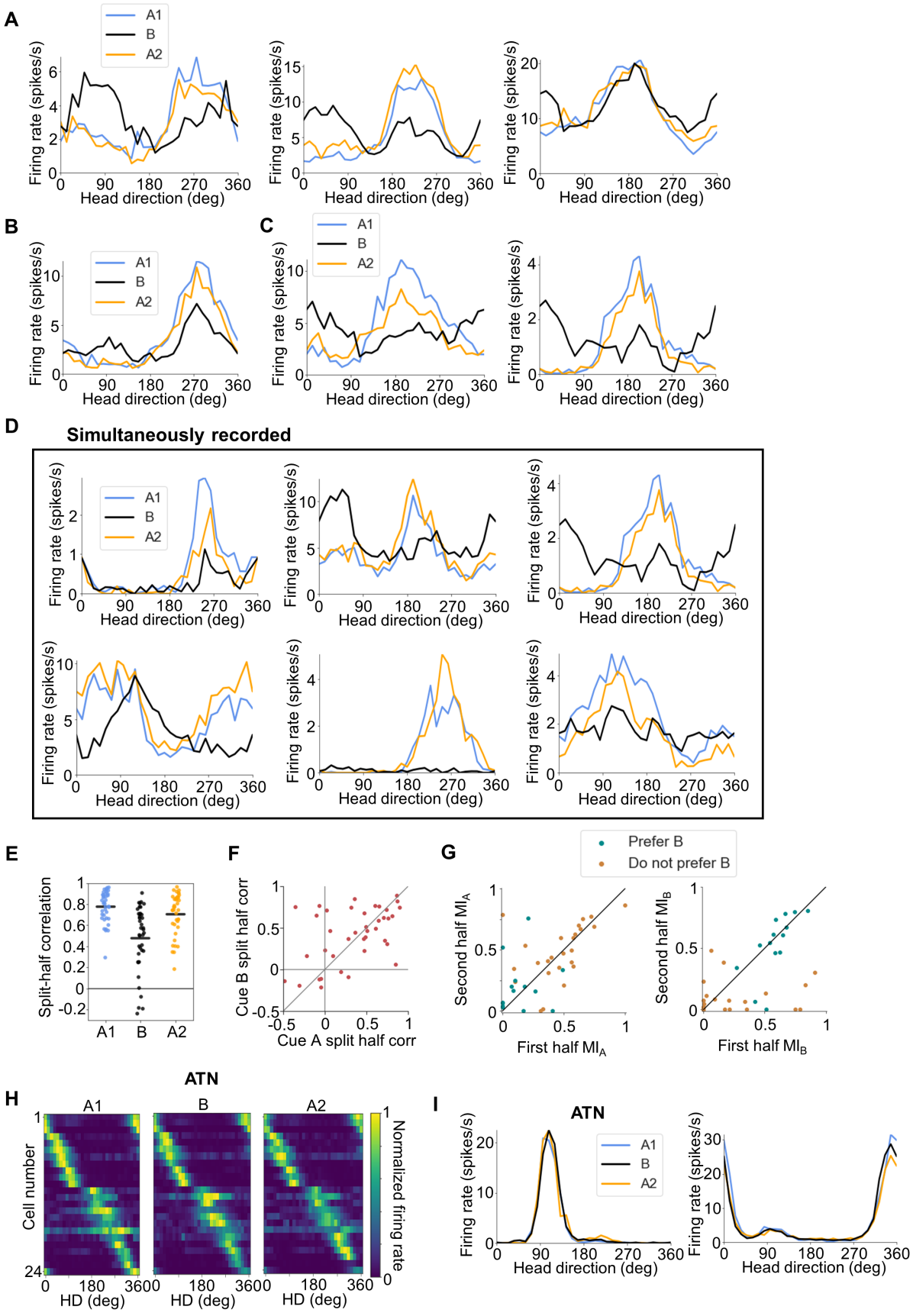
A
A1
B
A2
Firing rate (spikes/s)
Head direction (deg)
B
C
D
Simultaneously recorded
E
Split-half correlation
F
Cue B split half corr
Cue A split half corr
G
Prefer B
Do not prefer B
Second half MI$_A$
First half MI$_A$
Second half MI$_B$
First half MI$_B$
H
ATN
Cell number
HD (deg)
Normalized firing rate
I
ATN

Figure S9. B session additional data. (A) Tuning curves for three example POR LM-HD cells that showed strong bidirectionality in the B session. **(B)** Tuning curves for one example POR LM-HD cell that remained tuned primarily to the previous location of cue A in the B session. **(C)** Tuning curves for two example POR LM-HD cells that primarily encoded cue B in the B session. **(D)** Tuning curves for six simultaneously recorded POR LM-HD cells that showed a variety of responses to the B session. **(E)** Comparison of split-half correlations for all LM-HD cells recorded across the three sessions of the B experiment. **(F)** Comparison of split-half correlations between the portions of each cell's tuning curve related to each cue. **(G)** Comparison of tuning strength relative to the previous location of cue A (*left*) or cue B (*right*) using modulation index (MI) across both halves of the B session for all LM-HD cells recorded in the B session. Note that cells that 'preferred' cue B showed generally more stable tuning strength relative to cue B, while cells that did not 'prefer' cue B showed more stable tuning strength relative to cue A. **(H)** Normalized tuning curves for all ATN HD cells recorded in the B experiment. **(I)** Tuning curves for two example ATN HD cells recorded in the B experiment.

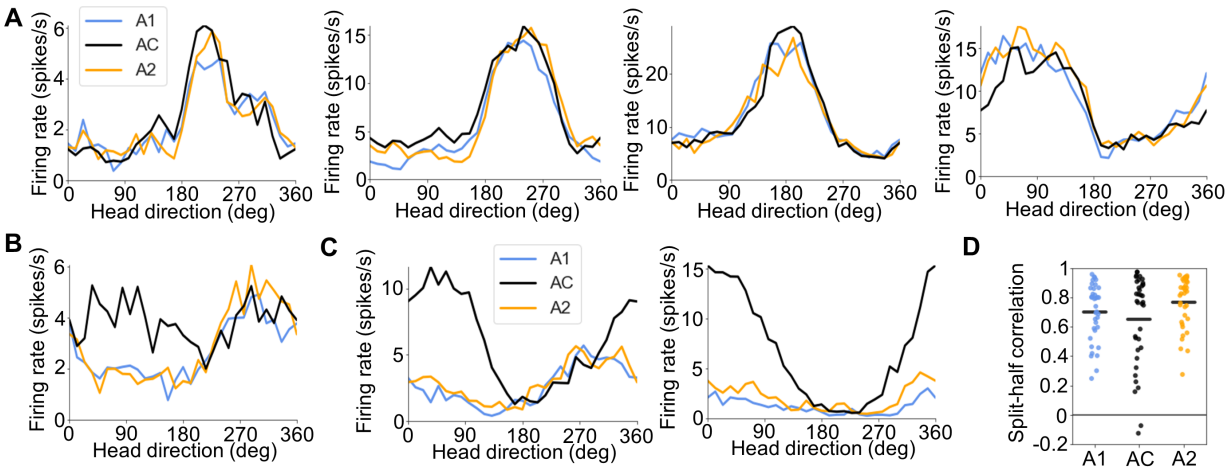

Figure S10. AC session additional data. (A) Tuning curves for four example POR LM-HD cells that remained unidirectional in the AC session. **(B)** Tuning curves for one example POR LM-HD cell that showed clear bidirectionality in the AC session. **(C)** Tuning curves for two example POR LM-HD cells that showed a strong increase in firing rate near 90° in the AC session, regardless of their A1 PFD. **(D)** Comparison of split-half correlations for all LM-HD cells recorded across the three sessions of the AC experiment.

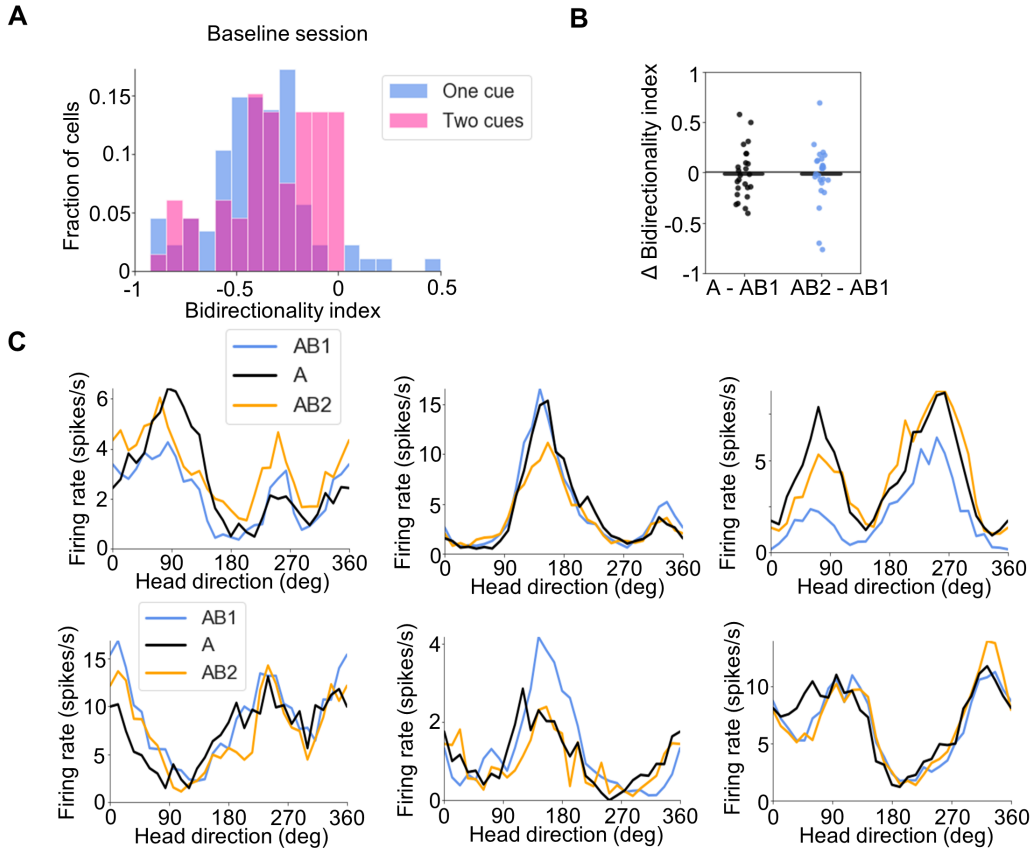

Figure S11. Bidirectionality among cells of animals trained with two identical cue cards. **(A)** Distribution of bidirectionality indices for all LM-HD cells from the A1 session of the initial AB experiment (trained with one white cue card) and all LM-HD cells from the AB1 session of the AB1-A-AB2 experiment (trained with two cue cards). Blue or pink indicates whether the animals were trained with one or two cues, respectively, while the purple color shows overlap between the two distributions. Note the large proportion of two-cue cells with BIs approaching 0. **(B)** Comparison of bidirectionality index between AB1 and both A and AB2 sessions for the 25 LM-HD cells with BI > -0.2 in the AB1 session. **(C)** Tuning curves for six POR LM-HD cells that showed mild bidirectionality in the AB1 condition that persisted throughout the sessions. Top row shows putative peak cells, bottom row shows putative trough cells.

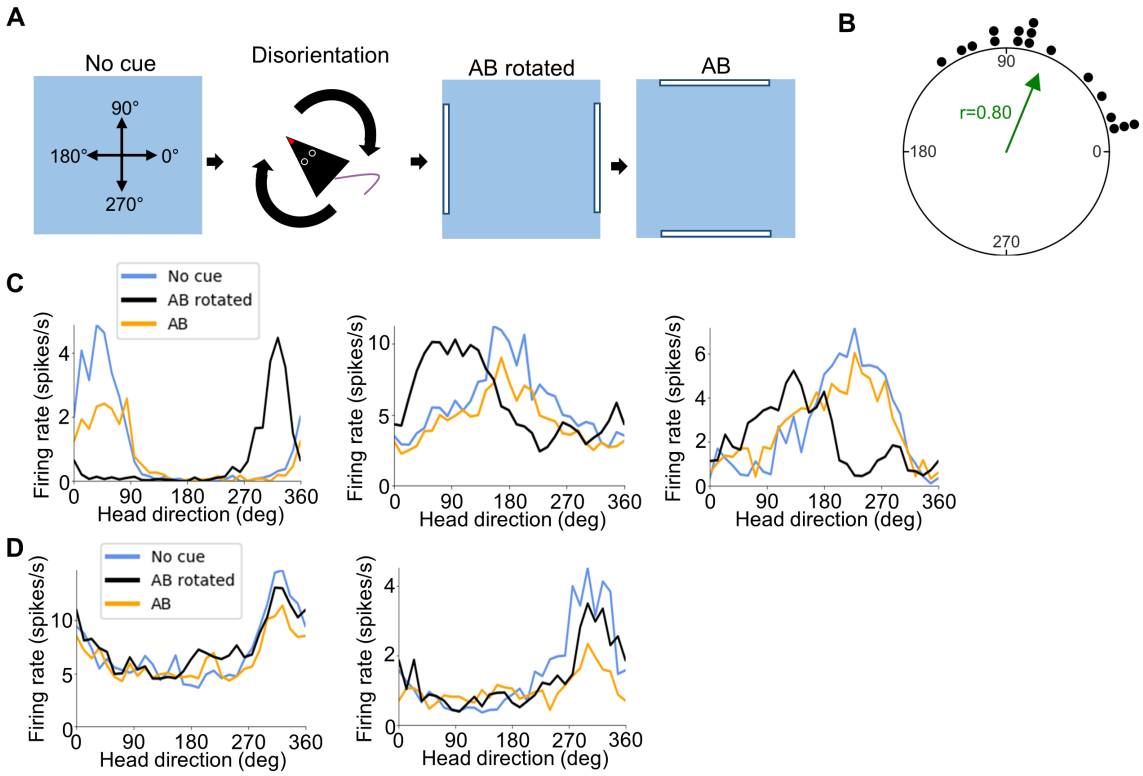

Figure S12. Effect of cue rotation on cells trained with no cues. (A) Experimental design for the cue rotation experiment. Top-down view of the recording arena showing the locations of visual cues across No cue, AB rotated, and AB sessions, as well as the reference frame for measuring allocentric head direction. Note that the animals were disoriented between the No cue and AB rotated sessions. **(B)** Absolute PFD shift for all 17 HD-responsive POR cells from the No cue session to the AB rotated session. Note that most cells (11/17) shifted their PFDs more than 45°, indicating that the cues were able to guide the cells' directional preferences despite their limited familiarity. **(C)** Tuning curves for three example HD-responsive POR cells that shifted their preferred directions along with the visual cues. **(D)** Tuning curves for two HD-responsive POR cells that did not shift their preferred directions.

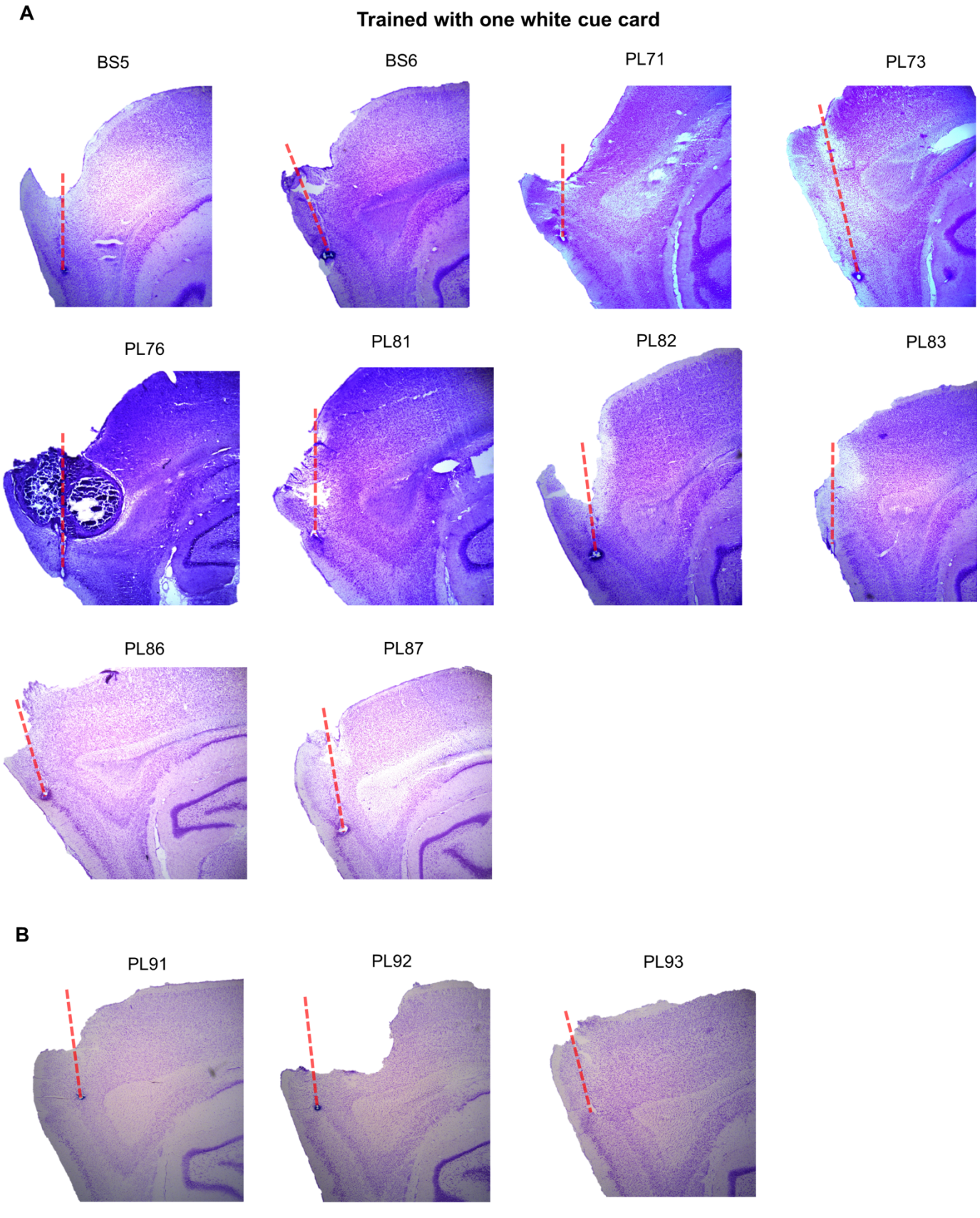
A
Trained with one white cue card
BS5
BS6
PL71
PL73
PL76
PL81
PL82
PL83
PL86
PL87
B
PL91
PL92
PL93

C

Trained with one black cue card

AM8

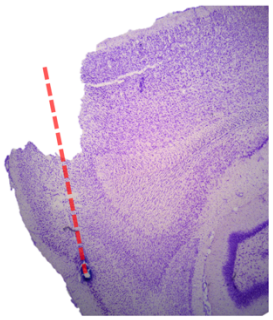

AM9

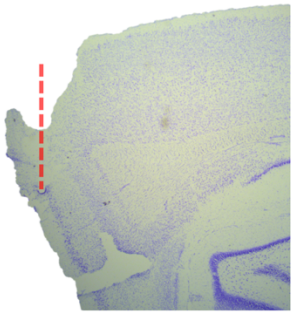

AM10

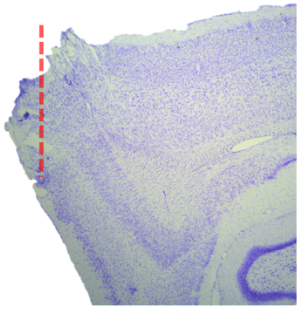

D

Trained with two white cue cards

PL88

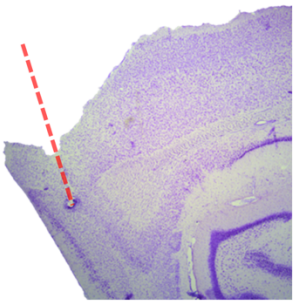

PL89

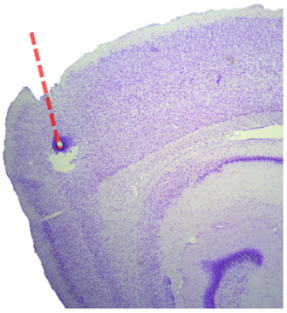

PL90

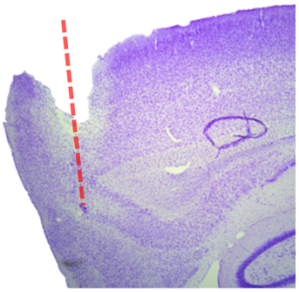

E

Trained with no cue cards

PL94

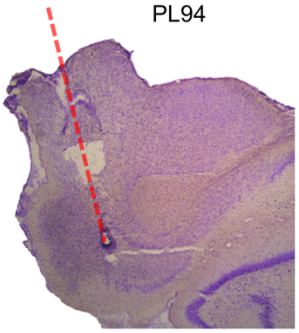

PL95

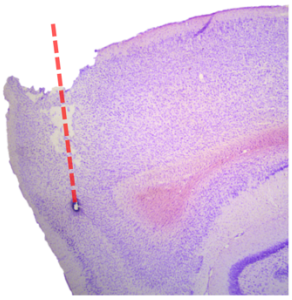

PL97

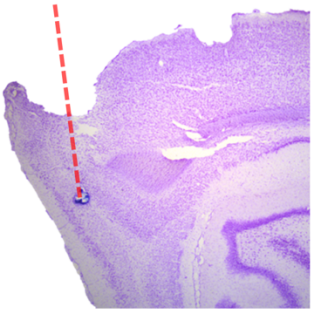

F

ATN animals – trained with one white cue card

BS1

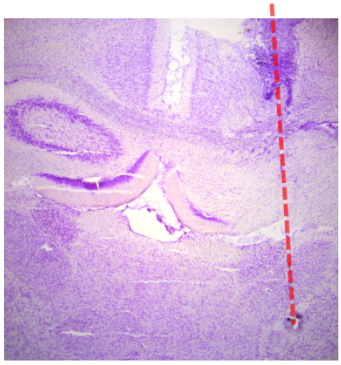

JG1

JG3

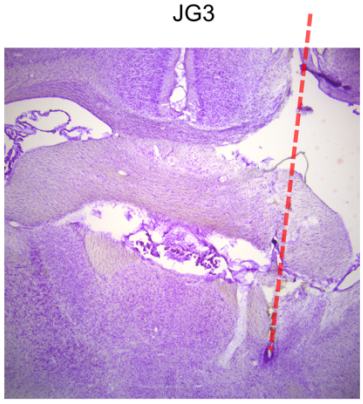

Figure S13. Histology. (A) Nissl stained sagittal slices for all POR-implanted rats initially implanted for the AB experiment. Red dashed lines denote cannula placement. Tracks all run through POR and end in either parasubiculum or entorhinal cortex. **(B)** Nissl stained sagittal slices for the three POR-implanted rats used in the A1-AB-No cue-A2 experiment. Tracks run through POR and end in either ventral POR or dorsal parasubiculum. **(C)** Nissl stained sagittal slices for the three POR-implanted rats trained with a single black cue card. Tracks run through POR and end in either parasubiculum or entorhinal cortex. **(D)** Nissl stained sagittal slices for the three POR-implanted rats trained with two identical white cue cards. Tracks run through POR and end in either POR, parasubiculum, or entorhinal cortex. **(E)** Nissl stained sagittal slices for the three POR-implanted rats trained with no cue cards. Tracks run through POR and end in either parasubiculum or entorhinal cortex. **(F)** Nissl stained coronal slices for all ATN-implanted rats used in the cue experiment. Red dashed lines denote cannula placement. Tracks run through either the anterodorsal (JG1, JG3) or anteroventral (BS1) thalamic nucleus.